A New Finite Element for Static and Dynamic Analysis of Cracked Composite Beams

Krawczuk, M.

Publication date:
1993

Document Version
Early version, also known as pre-print

INSTITUTTET FOR BYGNINGSTEKNIK
DEPT. OF BUILDING TECHNOLOGY AND STRUCTURAL ENGINEERING
AALBORG UNIVERSITETSCENTER • AUC • AALBORG • DANMARK

FRACTURE & DYNAMICS
PAPER NO. 43

Submitted to Int. Journal of Computers and Structures

M. KRAWCZUK
A NEW FINITE ELEMENT FOR STATIC AND DYNAMIC ANALYSIS OF CRACKED COMPOSITE BEAMS
JANUARY 1993 ISSN 0902-7513 R9305

The FRACTURE AND DYNAMICS papers are issued for early dissemination of research results from the Structural Fracture and Dynamics Group at the Department of Building Technology and Structural Engineering, University of Aalborg. These papers are generally submitted to scientific meetings, conferences or journals and should therefore not be widely distributed. Whenever possible reference should be given to the final publications (proceedings, journals, etc.) and not to the Fracture and Dynamics papers.

INSTITUTTET FOR BYGNINGSTEKNIK
DEPT. OF BUILDING TECHNOLOGY AND STRUCTURAL ENGINEERING
AALBORG UNIVERSITETSCENTER • AUC • AALBORG • DANMARK

FRACTURE & DYNAMICS
PAPER NO. 43

Submitted to Int. Journal of Computers and Structures

M. KRAWCZUK
A NEW FINITE ELEMENT FOR STATIC AND DYNAMIC ANALYSIS OF CRACKED COMPOSITE BEAMS
JANUARY 1993 ISSN 0902-7513 R9305

A NEW FINITE ELEMENT FOR STATIC AND DYNAMIC ANALYSIS OF CRACKED COMPOSITE BEAMS

(Submitted to An International Journal Computers & Structures)

MAREK KRAWCZUK
Institute of Fluid Flow Machinery, Polish Academy of Sciences
80-952 Gdansk, ul.Gen. J.Fiszera 14, Poland

Abstract - A new beam finite element with a single nonpropagating one-edge open crack located in its mid-length is formulated for static and dynamic analysis of cracked composite beam-like structures. The element includes two degrees of freedoms at each of the three nodes: a transverse deflection and an independent rotation respectively. The exemplary numerical calculations illustrating variations of static deformations and a fundamental bending natural frequency of composite cantilever beam caused by a single crack are presented. The element proves to be accurate and versatile. The compatibility with plate and shell elements as a stiffener is assured through the use of simple nodal variables of C^0-type. The presented method of creating the element makes it possible to construct beam finite elements with other types of cracks (double-edge, internal etc.) provided that stress intensity factors for a given type of crack are known.

A NEW FINITE ELEMENT FOR STATIC AND DYNAMIC ANALYSIS OF CRACKED COMPOSITE BEAMS

MAREK KRAWCZUK
Institute of Fluid Flow Machinery, Polish Academy of Sciences
80-952 Gdansk, ul.Gen. J.Fiszera 14, Poland

1. INTRODUCTION

High speed machinery and lightweight structures require high strength-to-weight ratios. For this reason, in recent years, the use of anisotropic reinforced composites, where strength-to-weight ratios is very high, has increased substantially in the fields of mechanical and civil engineering - see for example the textbook of Vinson and Chou [1].

Cracks occurring in structural elements are responsible for local stiffness variations [2], which in consequence affect their dynamic characteristics. This problem has been a subject of many papers, the review of which is given by Wauer [3], but only several papers has been devoted the changes of the dynamic characteristics of composite constructional elements. Adams *et al.* [4], found that damage in specimens fabricated from fiber reinforced plastics could be detected by reduction in natural frequencies and an increase in damping. Cawley and Adams [5], successfully tested the frequency measurement principle on composite structures made in the presence of damage. Nikpour and Dimarogonas [6], presented the local compliance matrix for unidirectional composite materials. They have shown that the interlocking deflection modes are enhanced as a function of the degree of anisotropy in composites. The effect of cracks upon buckling of an edge-notched column for isotropic and anisotropic composites has been studied by Nikpour [7]. He indicated that the instability increases with the column slenderness and the crack length. In addition he has shown that the material anisotropy conspicuously reduces the load-carrying capacity of an externally cracked member. Recently, Manivasagam and Chandrasekaran [8], have presented results of experimental investigations upon the reduction effect of the fundamental frequency of layered composite materials with damage in the form of cracks.

In the presented paper there has been made an attempt to work out a composite beam

finite element with nonpropagating one-edge open crack. It has been assumed that the crack changes only stiffness of the element whereas the mass of the element is unchanged. The element has been tested by numerical calculations, the results of which has been compared with results other investigators. The influence of the crack depth, the volume fraction of fiber and also the angle of fiber upon changes the static deflection and the fundamental natural frequency of the composite cantilever beam has been studied.

2. GENERAL DESCRIPTION OF THE NONCRACKED ELEMENT

The geometry of the presented element is shown in Fig.1. The element has three nodes at x=-0.5L, 0, 0.5L. At each node there are two degrees of freedom, which are the transverse displacements q_1, q_3, q_5 and independent rotations q_2, q_4, q_6.

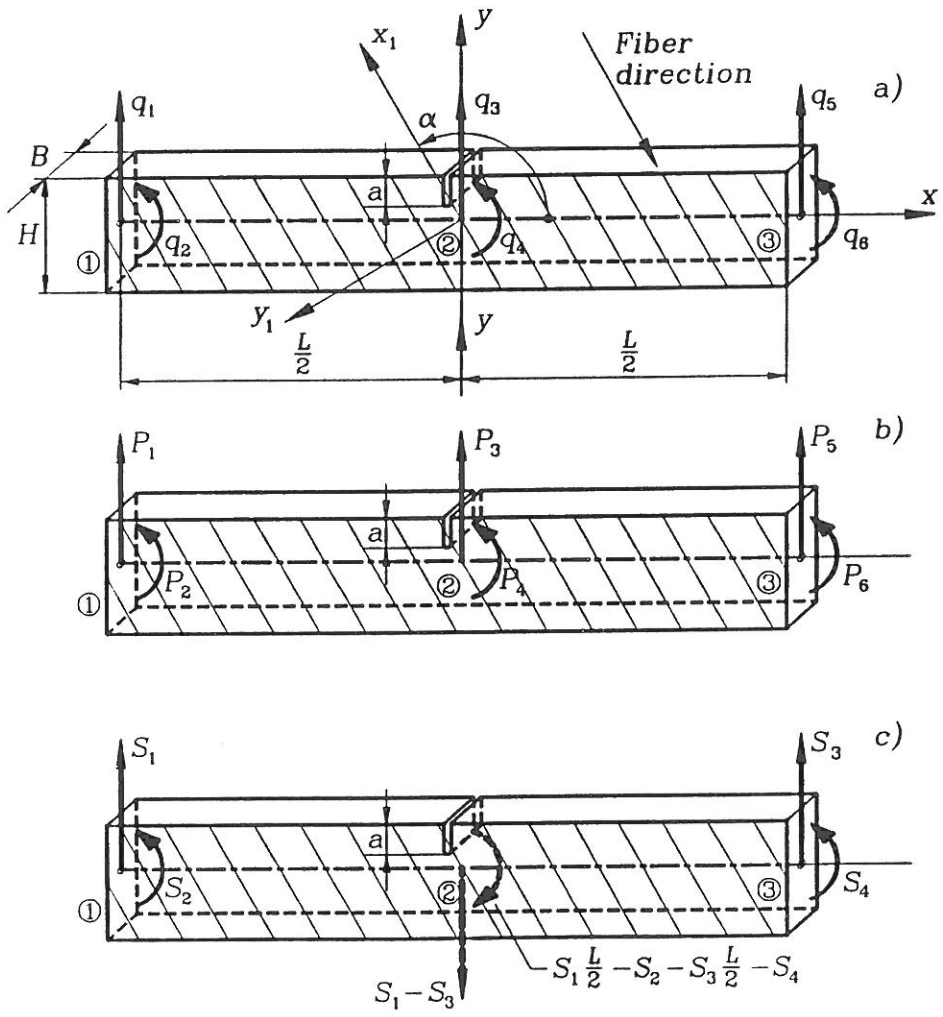

Fig.1

Neglecting warping the displacements u_x, u_y of a point of the element can be expressed as [9]

$$u_x(x,y) = -y\phi(x), \tag{1.a}$$

$$u_y(x,y) = v(x), \tag{1.b}$$

where $\phi(x)$ is the rotation and $v(x)$ denotes the transverse displacement.

Upon differentiation, the strains in the element are obtained as

$$\varepsilon_x = -y \frac{\partial \phi(x)}{\partial x}, \tag{2.a}$$

$$\gamma_{xy} = \frac{\partial v(x)}{\partial x} - \phi(x) . \tag{2.b}$$

In the finite element method, the transverse displacement $v(x)$ is assumed as cubic polynomials in x, while the independent rotation $\phi(x)$ can be expressed by quadratic polynomials. Hence, considering only the bending in the x-y plane the variables $v(x)$ and $\phi(x)$ are given by the following relations

$$v(x) = \beta_1 + \beta_2 x + \beta_3 x^2 + \beta_4 x^3, \tag{3.a}$$

$$\phi(x) = \beta_5 + \beta_6 x + \beta_7 x^2. \tag{3.b}$$

Assuming the shear strain variation to be linear as it proposed by Tessler and Dong [10], one receives relation between constant β_4 and β_7 in the form

$$\beta_7 = 3\beta_4, \tag{4}$$

hence, the transverse displacement $v(x)$ and the independent rotation $\phi(x)$ can be written as

$$v(x) = \beta_1 + \beta_2 x + \beta_3 x^2 + \beta_4 x^3, \tag{5.a}$$

$$\phi(x) = \beta_5 + \beta_6 x + 3\beta_4 x^2. \tag{5.b}$$

Take into account the boundary conditions at nodes of the element, the variables $v(x)$ and $\phi(x)$ can be expressed in terms of the element degrees of freedom

$$v(x)=q_3 + \left(-\frac{q_1}{L} - \frac{q_2}{6} + \frac{q_4}{3} + \frac{q_5}{L} - \frac{q_6}{6}\right)x + \left(\frac{2q_1}{L^2} - \frac{4q_3}{L^2} + \frac{2q_5}{L^2}\right)x^2 + \left(\frac{2q_2}{3L^2} - \frac{4q_4}{3L^2} + \frac{2q_6}{3L^2}\right)x^3, \tag{6.a}$$

$$\phi(x) = q_4 + \left(-\frac{q_2}{L} + \frac{q_6}{L}\right)x + \left(\frac{2q_2}{L^2} - \frac{4q_4}{L^2} + \frac{2q_6}{L^2}\right)x^2 , \tag{6.b}$$

Substitution relations (6.a-b) into (1.a-b) yields the displacements u_x, u_y of a point of the element in the form

$$\begin{pmatrix} u_x \\ u_y \end{pmatrix} = \mathbb{N} \begin{pmatrix} q_1 \\ \vdots \\ q_6 \end{pmatrix} , \tag{7}$$

where $\mathbb{N}$ denotes the shape function matrix of the element in the form

$$\mathbb{N} = \left[\begin{array}{c|c|c|c|c|c} 0 & (\frac{x}{L} - \frac{2x^2}{L^2})y & 0 & (\frac{4x^2}{L^2} - 1)y & 0 & -(\frac{2x^2}{L^2} + \frac{x}{L})y \\ \hline \frac{2x^2}{L^2} - \frac{x}{L} & \frac{2x^3}{3L^2} - \frac{x}{6} & 1 - \frac{4x^2}{L^2} & \frac{x}{3} - \frac{4x^3}{3L^2} & \frac{x}{L} + \frac{2x^2}{L^2} & \frac{2x^3}{3L^2} - \frac{x}{6} \end{array}\right], \tag{8}$$

In the similar fashion, substitution (6.a-b) into (2.a-b) yields the strains in terms of the element degrees of freedom as

$$\begin{pmatrix} \varepsilon_x \\ \gamma_{xy} \end{pmatrix} = \mathbb{B} \begin{pmatrix} q_1 \\ \vdots \\ q_6 \end{pmatrix} , \tag{9}$$

where $\mathbb{B}$ denotes the strains-nodal displacements relation matrix in the form

$$\mathbb{B} = \left[\begin{array}{c|c|c|c|c|c} 0 & \frac{y}{L} - \frac{4xy}{L^2} & 0 & \frac{8xy}{L^2} & 0 & -\frac{4xy}{L^2} - \frac{y}{L} \\ \hline \frac{4x}{L^2} - \frac{1}{L} & \frac{x}{L} - \frac{1}{6} & -\frac{8x}{L^2} & -\frac{2}{3} & \frac{1}{L} + \frac{4x}{L^2} & -\frac{x}{L} - \frac{1}{6} \end{array}\right], \tag{10}$$

3. INERTIA MATRIX OF THE CRACKED ELEMENT

Because, it has been assumed that the crack occurring in the element not change the mass of its, the inertia matrix has the same form like in the case of the noncracked one.

The inertia matrix of the noncracked element $\mathbb{M}_e$ is calculating from the commonly known equation, Zienkiewicz [11]

$$\mathbb{M}_e = \rho \int_v \mathbb{N}^T \mathbb{N} \, dv, \tag{11}$$

where ρ is the mass density and v is the volume of the element.

Substitution (8) into (11) yields the inertia matrix of the presented element in the closed form

$$\mathbb{M}_e = \frac{\rho BHL}{3780} \left[\begin{array}{c|c|c|c|c|c} 504 & & & & & \\ \hline 21L & 42H^2+2L^2 & & & \text{sym.} & \\ \hline 252 & 0 & 2016 & & & \\ \hline -42L & 21H^2-4L^2 & 0 & 168H^2+8L^2 & & \\ \hline -126 & -21L & 252 & 42L & 504 & \\ \hline 21L & -10.5H^2+2L^2 & 0 & 21H^2-4L^2 & -21L & 42H^2+2L^2 \end{array}\right] \tag{12}$$

where B,H,L are dimensions of the element shown in Fig.1.

4. STIFFNESS MATRIX OF THE CRACKED ELEMENT

The stiffness matrix $\mathbb{K}_e$ of the finite element can be calculated by means of the relation, Przemieniecki [12]

$$\mathbb{K}_e = \mathbb{T}^t \, \mathbb{C}^{-1} \, \mathbb{T}, \tag{13}$$

where $\mathbb{T}$ is the transformation matrix of a system of dependent nodal forces P_i (i=1,6) into the system of independent nodal forces S_i (i=1,4) - see Fig.1, $\mathbb{C}^{-1}$ is the inverse of flexibility matrix of the element, t denotes transpose of the matrix.

In the case of the cracked element the flexibility matrix $\mathbb{C}$ is represented by a sum of the flexibility matrix of the noncracked element $\mathbb{C}^o$ and the additional flexibility matrix $\mathbb{C}^1$ caused by the crack

$$\mathbb{C} = \mathbb{C}^o + \mathbb{C}^1, \tag{14}$$

5. MATRIX OF TRANSFORMATION

The matrix of transformation $\mathbb{T}$ is calculated using the equation of overall equilibrium for element forces P_i (i=1,6) and S_i (i=1,4) - see Fig.1. The finally form of this matrix can be presented in the following form

$$\mathbb{T}^t = \begin{bmatrix} 1 & 0 & 0 & 0 \\ 0 & 1 & 0 & 0 \\ -1 & 0 & -1 & 0 \\ L/2 & -1 & -L/2 & -1 \\ 0 & 0 & 1 & 0 \\ 0 & 0 & 0 & 1 \end{bmatrix}, \tag{15}$$

6. FLEXIBILITY MATRIX OF THE NONCRACKED ELEMENT

The terms of the flexibility matrix of the noncracked element $\mathbb{C}^o$ can be determined by inversion of the force-displacement equation, Przemieniecki [12]. For the presented element the force-displacement equation has the form

$$\begin{bmatrix} P_1 \\ P_2 \\ P_3 \\ P_4 \\ P_5 \\ P_6 \end{bmatrix} = \begin{bmatrix} k_{11} & k_{12} & k_{13} & k_{14} & k_{15} & k_{16} \\ k_{21} & k_{22} & k_{23} & k_{24} & k_{25} & k_{26} \\ k_{31} & k_{32} & k_{33} & k_{34} & k_{35} & k_{36} \\ k_{41} & k_{42} & k_{43} & k_{44} & k_{45} & k_{46} \\ k_{51} & k_{52} & k_{53} & k_{54} & k_{55} & k_{56} \\ k_{61} & k_{62} & k_{63} & k_{64} & k_{65} & k_{66} \end{bmatrix} \begin{bmatrix} q_1 \\ q_2 \\ q_3 \\ q_4 \\ q_5 \\ q_6 \end{bmatrix}, \tag{16}$$

According with Fig.1 the second node of the element is constrained i.e.

$$q_3 = q_4 = 0, \tag{17}$$

Applying the condition (17), the equation (16) can be transformed to the inversion form

$$\begin{bmatrix} q_1 \\ q_2 \\ q_5 \\ q_6 \end{bmatrix} = \begin{bmatrix} k_{11} & k_{12} & k_{15} & k_{16} \\ k_{21} & k_{22} & k_{25} & k_{26} \\ k_{51} & k_{52} & k_{55} & k_{56} \\ k_{61} & k_{62} & k_{65} & k_{66} \end{bmatrix}^{-1} \begin{bmatrix} P_1 \\ P_2 \\ P_5 \\ P_6 \end{bmatrix} \tag{18}$$

Finally, the flexibility matrix of the noncracked element under a selected independent system is

$$\mathbb{C}^o = \begin{bmatrix} k_{11} & k_{12} & k_{15} & k_{16} \\ k_{21} & k_{22} & k_{25} & k_{26} \\ k_{51} & k_{52} & k_{55} & k_{56} \\ k_{61} & k_{62} & k_{65} & k_{66} \end{bmatrix}^{-1}. \tag{19}$$

The terms k_{ij} are equal to terms of the stiffness matrix of the noncracked element $\mathbb{K}_e$, which is calculated according with the following formula, Zienkiewicz [11]

$$\mathbb{K}_e = \int_V \mathbb{B}^T \, \mathbb{D} \, \mathbb{B} \, dv, \tag{20}$$

where $\mathbb{D}$ denotes the stresses-strains relation matrix - see Appendix C.

Substitution (10) into (20) yields the terms of the stiffness matrix of the noncracked element in the form

$$k_{11} = k_{55} = 7BH\bar{S}_{33}/3L \ ,$$

$$k_{12} = k_{21} = -k_{56} = -k_{65} = BH\bar{S}_{33}/2 \ ,$$

$$k_{13} = k_{31} = k_{35} = k_{53} = -8BH\bar{S}_{33}/3L \ ,$$

$$k_{14} = k_{41} = k_{36} = k_{63} = -k_{23} = -k_{32} = -k_{45} = -k_{54} = 2BH\bar{S}_{33}/3 \ ,$$

$$k_{15} = k_{51} = BH\bar{S}_{33}/3L \ ,$$

$$k_{16} = k_{61} = -k_{25} = -k_{52} = -BH\bar{S}_{33}/6 \ ,$$

$$k_{22} = k_{66} = BH(7H^2\bar{S}_{11}/36L + L\bar{S}_{33}/9) \ ,$$

$$k_{24} = k_{42} = k_{46} = k_{64} = BH(-2H^2\bar{S}_{11}/9L + L\bar{S}_{33}/9) \ ,$$

$$k_{26} = k_{62} = BH(H^2\bar{S}_{11}/36L - L\bar{S}_{33}/18) \ ,$$

$$k_{33} = 16BH\bar{S}_{33}/3L \ ,$$

$$k_{44} = BH(4H^2\bar{S}_{11}/9L + 4L\bar{S}_{33}/9) \ ,$$

$$k_{34} = k_{43} = 0.$$

where the form $\bar{S}_{11}$ and $\bar{S}_{33}$ is given in the Appendix C.

7. ADDITIONAL FLEXIBILITY MATRIX OF THE ELEMENT DUE TO THE CRACK

The terms of the additional flexibility matrix $\mathbb{C}^1$ due to the crack are calculated making use of the relation

$$c_{ij}^1 = \frac{\partial^2 U^1}{\partial S_i \partial S_j} , \tag{21}$$

where U^1 is the additional elastic strain energy of the element caused by the crack, S_i, S_j are independent nodal forces acting on the element.

The additional elastic strain energy U^1 due to the presence of the crack in the analyzed element can be expressed as a function of the stress intensity factors [6]

$$U^1 = \int_A \left(D_1 \sum_{i=1}^{i=4} K_{IIi}^2 + D_{12} \sum_{i=1}^{i=4} K_{IIi} \sum_{i=1}^{i=4} K_{IIIi} + D_2 \sum_{i=1}^{i=4} K_{IIIi}^2 \right) dA \tag{22}$$

where A is the area of the crack, K_{IIi}, K_{IIIi} are the stress intensity factors corresponding with two models of the crack evaluation, i denotes independent nodal forces acting on the element, and the coefficients D_1, D_{12} and D_2 are given by the following relations [6]

$$D_1 = - 0.5\bar{b}_{22} \mathrm{Im}\left(\frac{s_1+s_2}{s_1 s_2} \right) , \tag{23.a}$$

$$D_{12} = \bar{b}_{11} \mathrm{Im}\left(s_1 s_2 \right) , \tag{23.b}$$

$$D_2 = 0.5\bar{b}_{11} \mathrm{Im}\left(s_1 + s_2 \right) . \tag{23.c}$$

The method of calculation the terms s_1, s_2 and $\bar{b}_{ij}$ is shown in the Appendix B. The variations of coefficients D_1, D_{12} and D_2 versus the fiber volume fraction and the crack angle are presented in Figs.2-4.

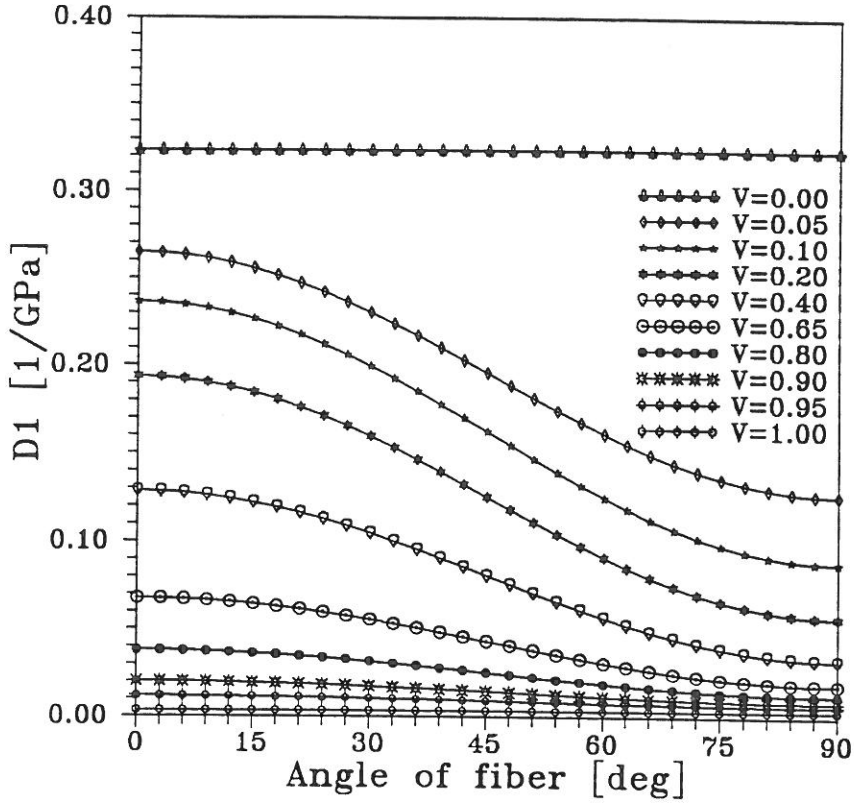
0.40
0.30
0.20
0.10
0.00
D1 [1/GPa]
V=0.00
V=0.05
V=0.10
V=0.20
V=0.40
V=0.65
V=0.80
V=0.90
V=0.95
V=1.00
0
15
30
45
60
75
90
Angle of fiber [deg]

Fig.2

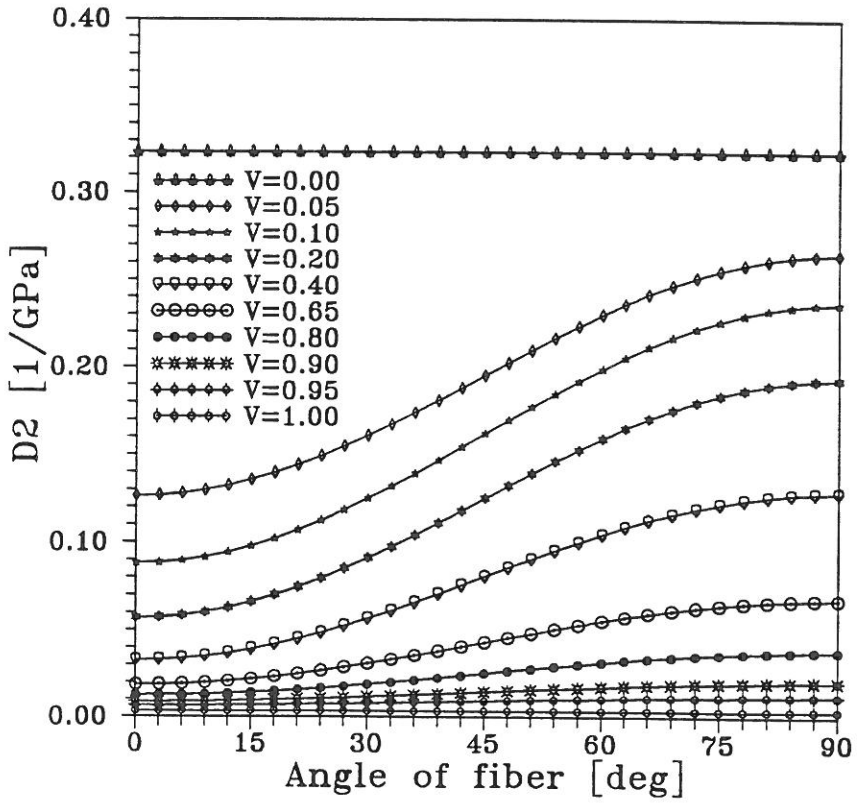
0.40
0.30
0.20
0.10
0.00
D2 [1/GPa]
V=0.00
V=0.05
V=0.10
V=0.20
V=0.40
V=0.65
V=0.80
V=0.90
V=0.95
V=1.00
0
15
30
45
60
75
90
Angle of fiber [deg]

Fig.3

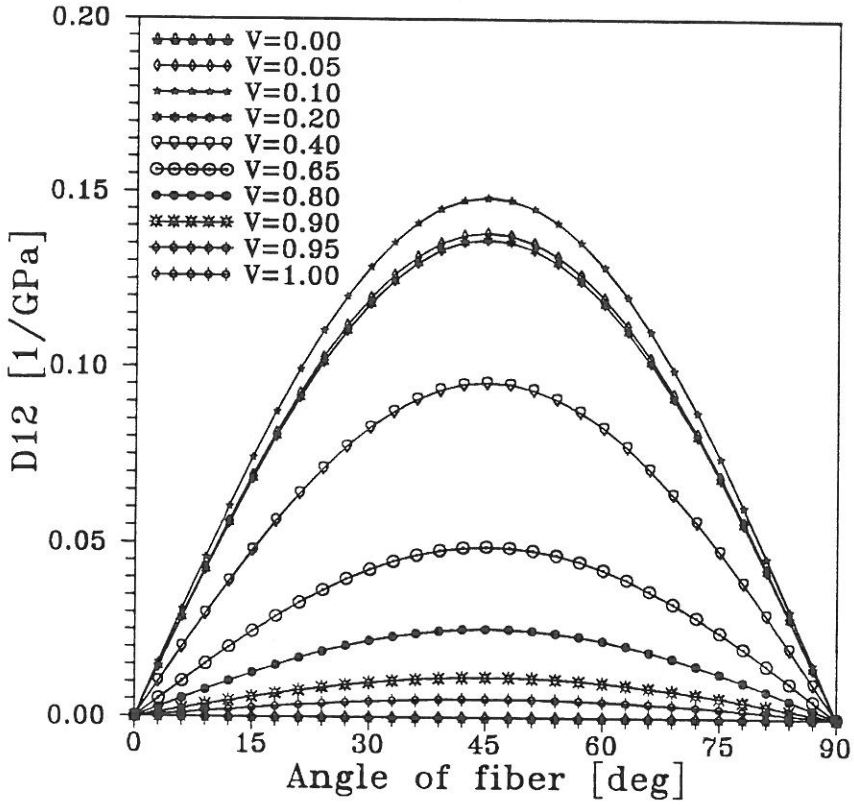

Fig.4

The stress intensity factors can be expressed as a function of independent nodal forces (Krawczuk and Ostachowicz [13], and also Krawczuk [14]). Generally, for anisotropic materials, the stress intensity factors are not equivalent to those of isotropic bodies of the same geometry and loading conditions, expect when the crack tips are sufficiently far away from loading points and the edges of specimen.

For the one-edge crack the nonzero stress intensity factors in function of independent nodal forces are equal

$$K_{I2} = \frac{6S_2}{BH^2} \sqrt{\pi a}\, Y_1 \,, \tag{24.a}$$

$$K_{I4} = \frac{6S_4}{BH^2} \sqrt{\pi a}\, Y_1 \,, \tag{24.b}$$

$$K_{II1} = \frac{S_1}{BH} \sqrt{\pi a}\, Y_2 \tag{24.c}$$

$$K_{II3} = \frac{S_3}{BH} \sqrt{\Pi a}\, Y_2 \ , \tag{24.d}$$

where a is the crack depth, Y_1 and Y_2 are correction factors.

The correction factors Y_1 and Y_2 arise from the lack of symmetry and the deformation at the free edges of the beam compared with an infinite plate containing a crack. These factors are nondimensional functions of the relative depth of crack ($\bar{a}$=a/H) and the anisotropic constants of material which may be expressed in terms of the roots of the characteristic equation (Appendix B). In many cases, however, the numerical analysis of highly anisotropic materials demonstrates a very weak correlation between the material anisotropic constants and Y-factors. Denoting these anisotropic perturbations by $C_1(\zeta)$, the Y-factors for isotropic materials given by Tada *et al.* [15], can be expressed as

$$Y_1 = \sqrt{\tan\lambda/\lambda}\,[0.923 + 0.199(1-\sin\lambda)^4]C_1(\zeta)/\cos\lambda \ , \tag{25.a}$$

$$Y_2 = (1.122 - 0.561\bar{a} + 0.085\bar{a}^2 + 0.18\bar{a}^3)/\sqrt{1 - \bar{a}}, \tag{25.b}$$

where $\lambda = \Pi\bar{a}/2$.

The factor $C_1(\zeta)$ for the edge-notched beam can be fitted by a single function [16]

$$C_1(\zeta) = 1.0 + 0.1(\zeta-1) - 0.16(\zeta-1)^2 + 0.002(\zeta-1)^3 \ . \tag{26}$$

where $\zeta = \dfrac{\sqrt{E_{11}E_{22}}}{2G_{12}} - \nu_{12}$, (the material constants E_{11}, E_{22}, G_{12} and ν_{12} are described in Appendix A).

Substitution relations (24.a-d), (25.a-b) and (26) into (22) yields the additional flexibility matrix of the element due to the crack as

$$\mathbb{C}^1 = \begin{bmatrix} c_{11} & c_{12} & c_{13} & c_{14} \\ & c_{22} & c_{23} & c_{24} \\ & & c_{33} & c_{34} \\ \text{sym.} & & & c_{44} \end{bmatrix} \tag{27}$$

where the following terms of the matrix are equal

$$c_{11} = c_{13} = c_{33} = \frac{2\Pi D_2}{B} \int_0^{\bar{a}} \bar{a}\, Y_2^2\, d\bar{a} ,$$

$$c_{22} = c_{24} = c_{44} = \frac{72\Pi D_1}{BH^2} \int_0^{\bar{a}} \bar{a}\, Y_1^2\, d\bar{a} ,$$

$$c_{12} = c_{14} = c_{23} = c_{34} = \frac{6\Pi D_{12}}{BH} \int_0^{\bar{a}} \bar{a}\, Y_1 Y_2\, d\bar{a} .$$

The changes of integrals as a function of the relative depth of the crack, for graphite-fiber reinforced polyimide from Appendix A (volume fraction of fiber - 10%), are presented in Fig.5.

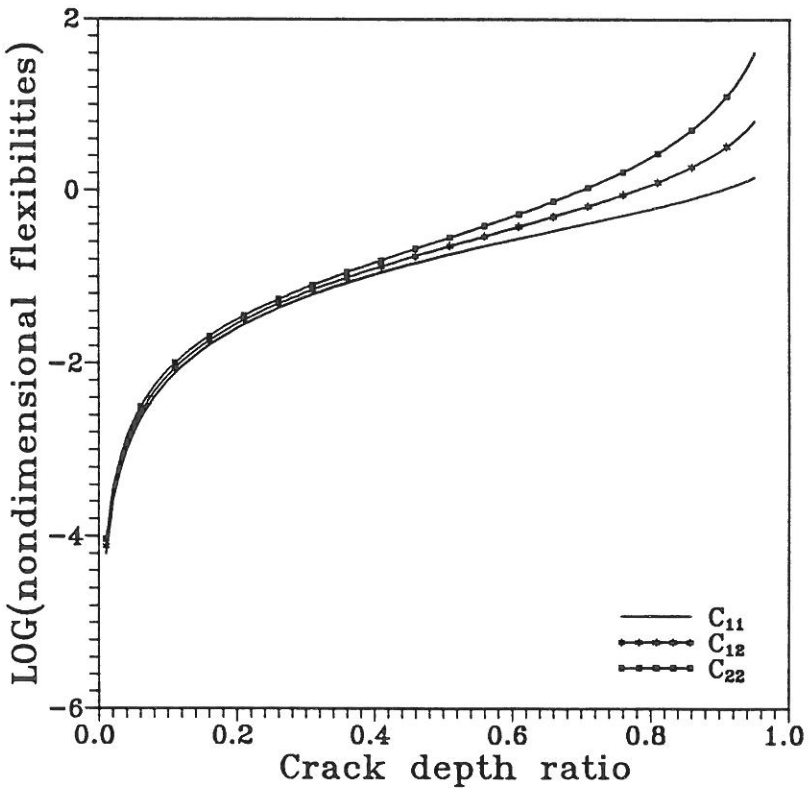

Fig.5

8. NUMERICAL STUDIES

The formulation of the element have been evaluated by performing the following examples.

1. Static deflection of the noncracked composite cantilever beam

The noncracked composite cantilever beam shown in Fig.6 is subjected to bending force. The material properties of graphite-fiber reinforced polyimide used in the analysis are given in the Appendix A. The calculations were carried out for various values of the angle of fiber and the volume fraction of fiber V.

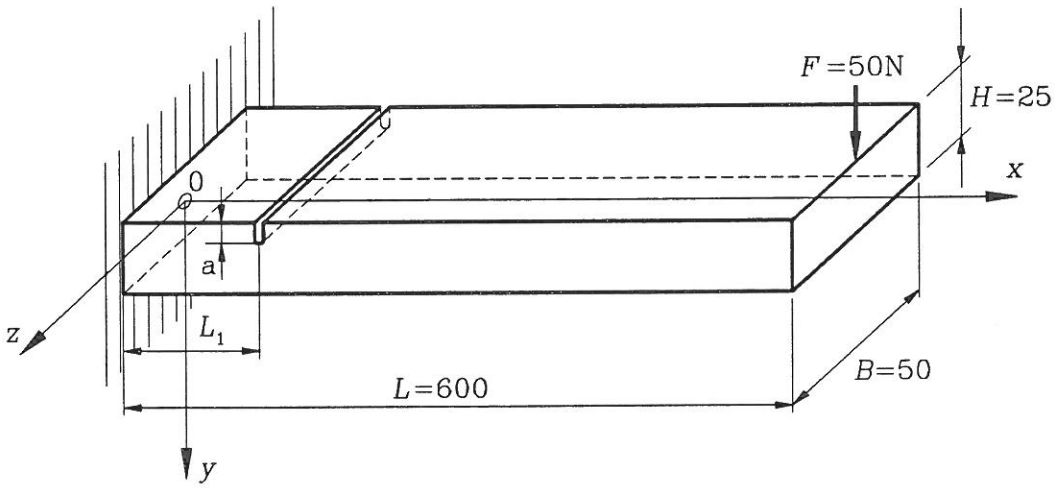

Fig.6

The static deflection of the end of beam obtained by a four element model is compared with analytical solution of Lekhnitskii [17], in Fig.7. It is noted that for all values of the fiber volume fraction V and the fiber angle results are in excellent agreement.

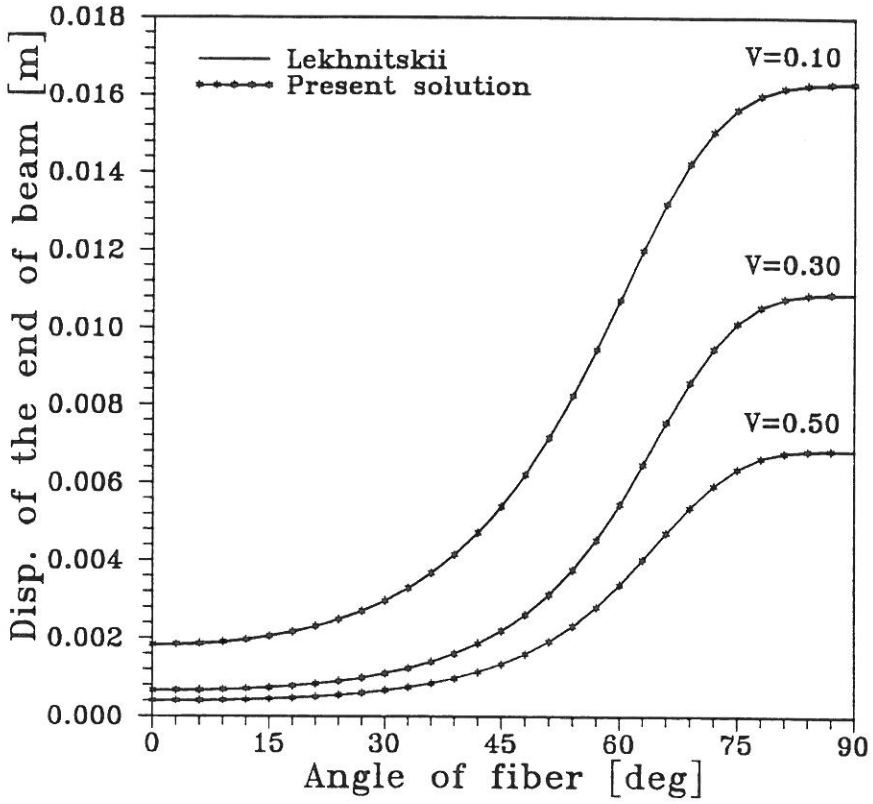

Fig.7

2. Static deflection of the cracked composite cantilever beam

The second example was carried out for the cracked composite cantilever beam with the same material properties and dimensions like in the point 1. The nonpropagating one-edge open crack is located 75 mm from the fixed end of the beam. The depth of the crack is various, equal to 0.2, 0.4 and 0.6 of the height of beam, respectively. The model of the beam contains three noncracked beam elements and one element with crack.

Fig.8 shows the relative static deflections of the end of beam as a function of the fiber angle and the relative depth of the crack a/H, for various values of the fiber volume fraction. The relative static deflection is calculating as

$$f_r = \frac{f_c(\alpha)}{f_{nc}(\alpha)} , \tag{28}$$

where $f_c(\alpha)$ denotes the static deflection of the cracked beam as a function of the angle of

fiber, $f_{nc}(\alpha)$ denotes the static deflection of the noncracked beam as a function of the angle of fiber, α is the angle of fiber.

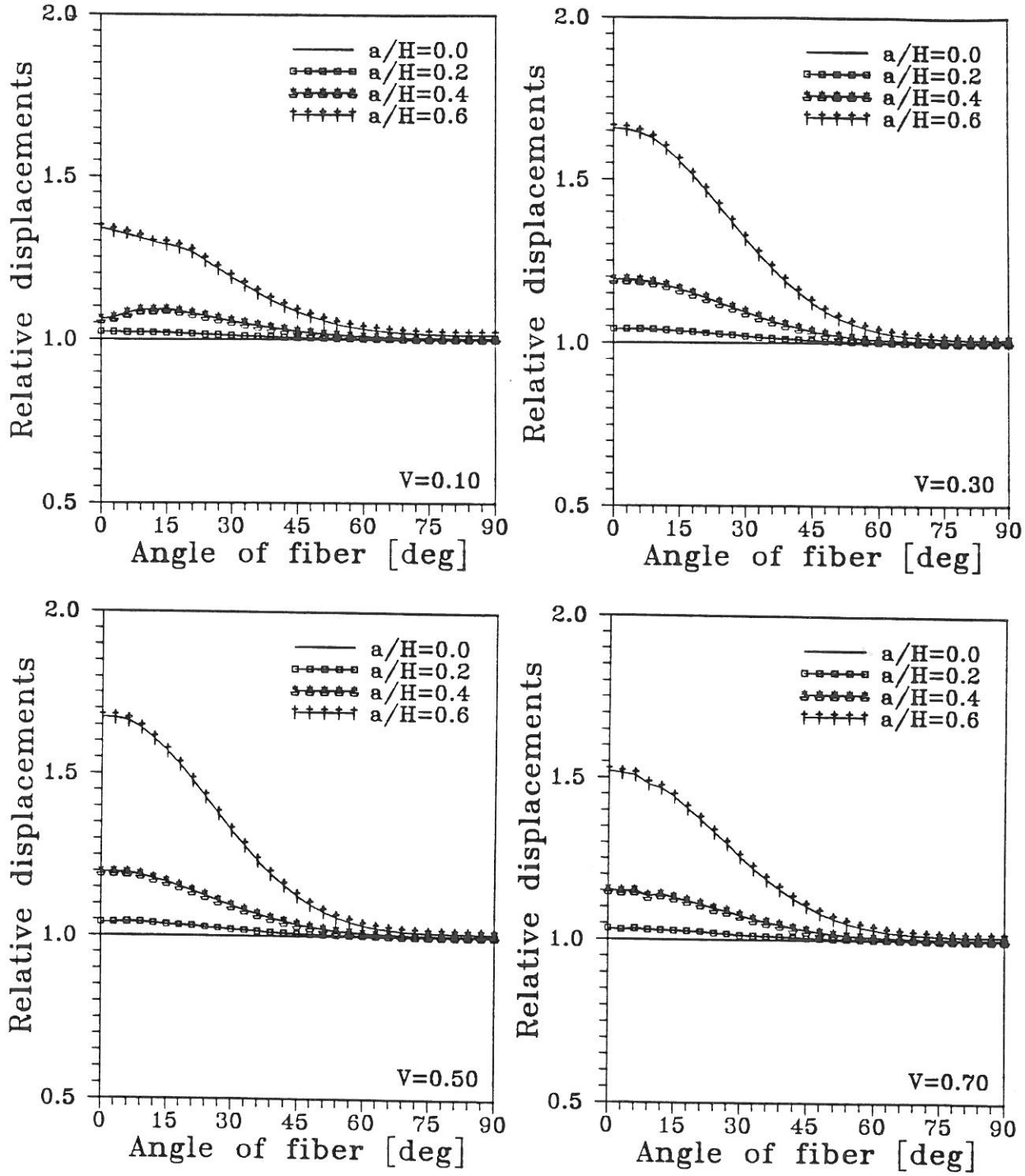

Fig.8

The maximum value of the relative static deflection is observed for the crack perpendiculars to fibers of the composite. When the fiber angle increases the relative static deflection is reduced and practically for the angle greater than 45 deg. the static deflection (even for relatively depth crack a/H=0.4), has the same value like in the case of the noncracked beam.

Fig.9 shows the influence of the volume fraction of fiber on the relative static deflections of the analyzed beam. In this case, the relative static deflection of the beam is calculating as

$$f_r = \frac{f_c(V)}{f_{nc}(V)}, \tag{29}$$

where $f_c(V)$ denotes the static deflection of the cracked beam as a function of the volume fraction of fiber, $f_{nc}(V)$ denotes the static deflection of the noncracked beam as a function of the volume fraction of fiber, V is the volume fraction of fiber.

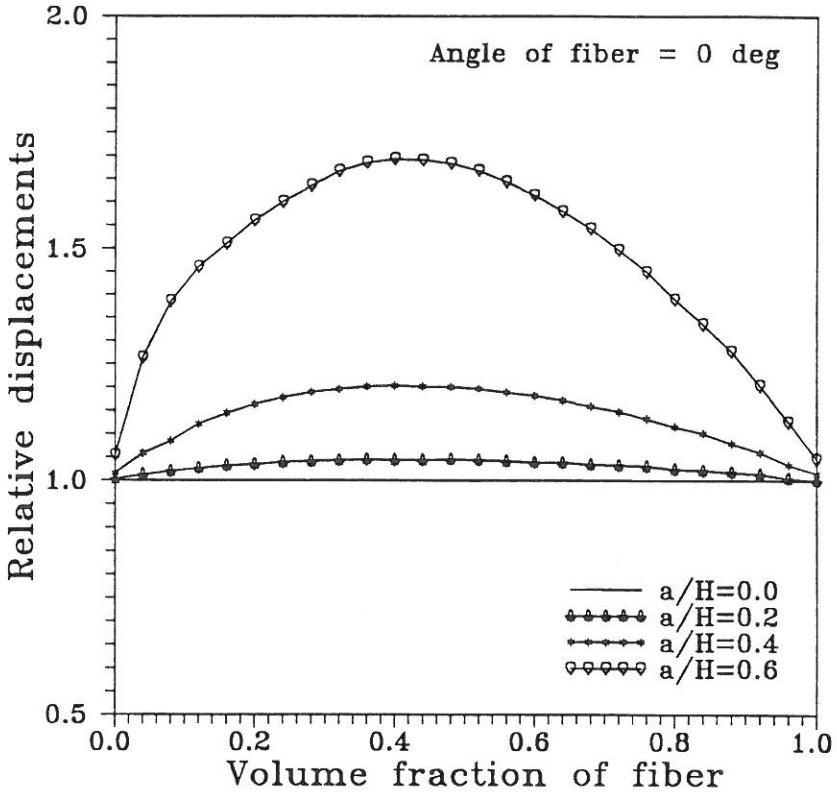

Fig.9

The relative static deflection is strongly dependent on the volume fraction of fiber. The maximum value is achieved at relatively higher fiber fractions (around 40%).

3. Natural frequencies of the noncracked composite cantilever beam

In this point the bending natural frequencies of the noncracked composite beam from example 1 were determined. The calculations were carried out for various values of the angle of fiber and the fiber volume fraction V.

The first three nondimensional bending natural frequencies obtained by a four element model are compared with analytical solution given by Vinson and Sierakowski [18], in Fig.10. The frequencies are normalized according with the relation

$$\bar{\omega} = l \sqrt{\omega h \,/\, \sqrt{\bar{S}_{11}/12\rho}} \quad , \tag{30}$$

where l is the length of the beam, h denotes the height of the beam and ω is the dimensional natural frequency.

It is noted that for first free natural frequencies results are in satisfactory agreement.

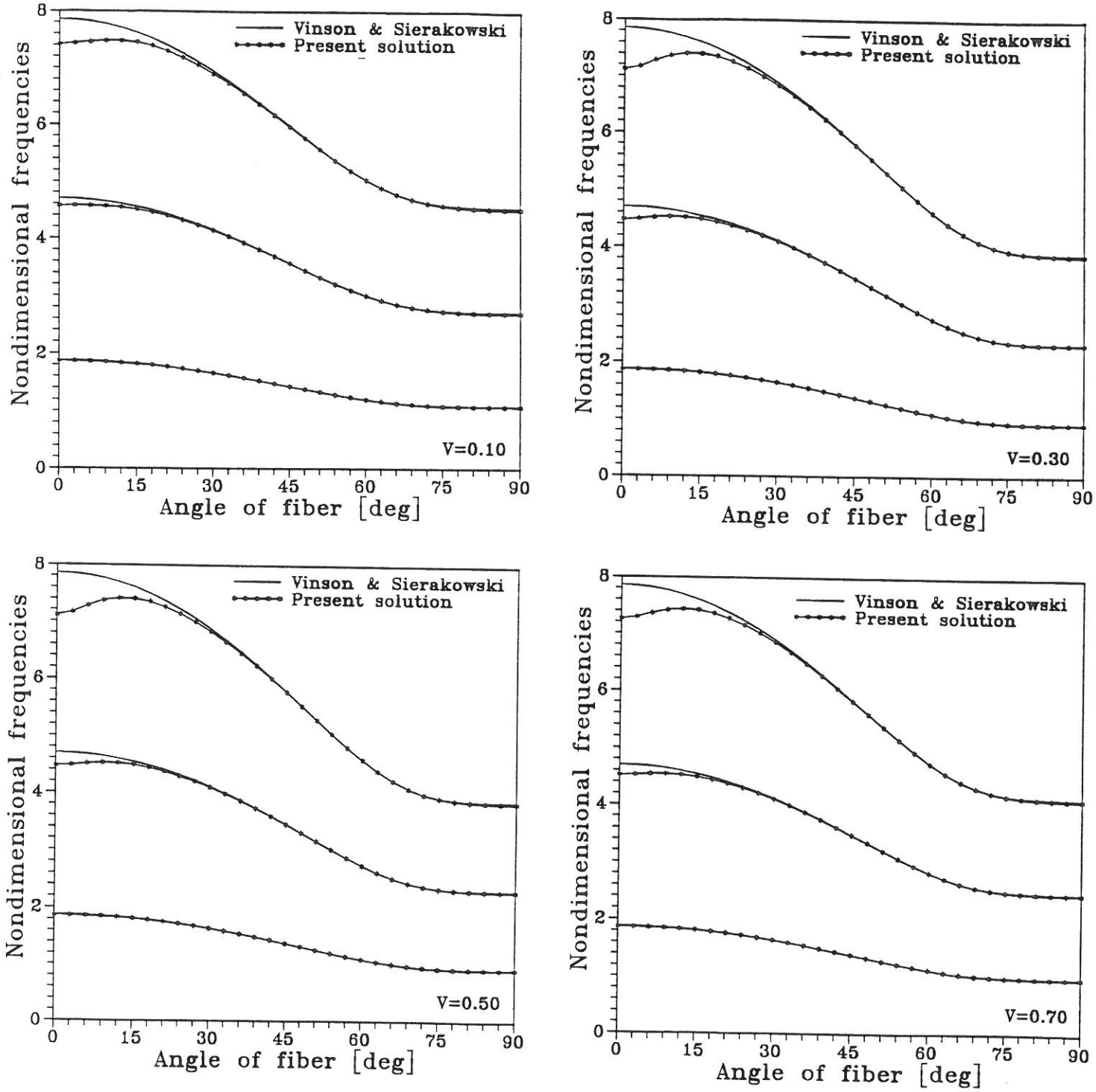

Fig.10

4. Natural frequencies of the cracked composite cantilever beam

The last example is devoted to analyze the change of the bending natural frequencies of the cracked composite beam from example 2. The calculations were carried out for various

value of the fiber volume fraction, the fiber angle and the depth of the crack. The model of the beam contains three noncracked beam elements and one element with crack.

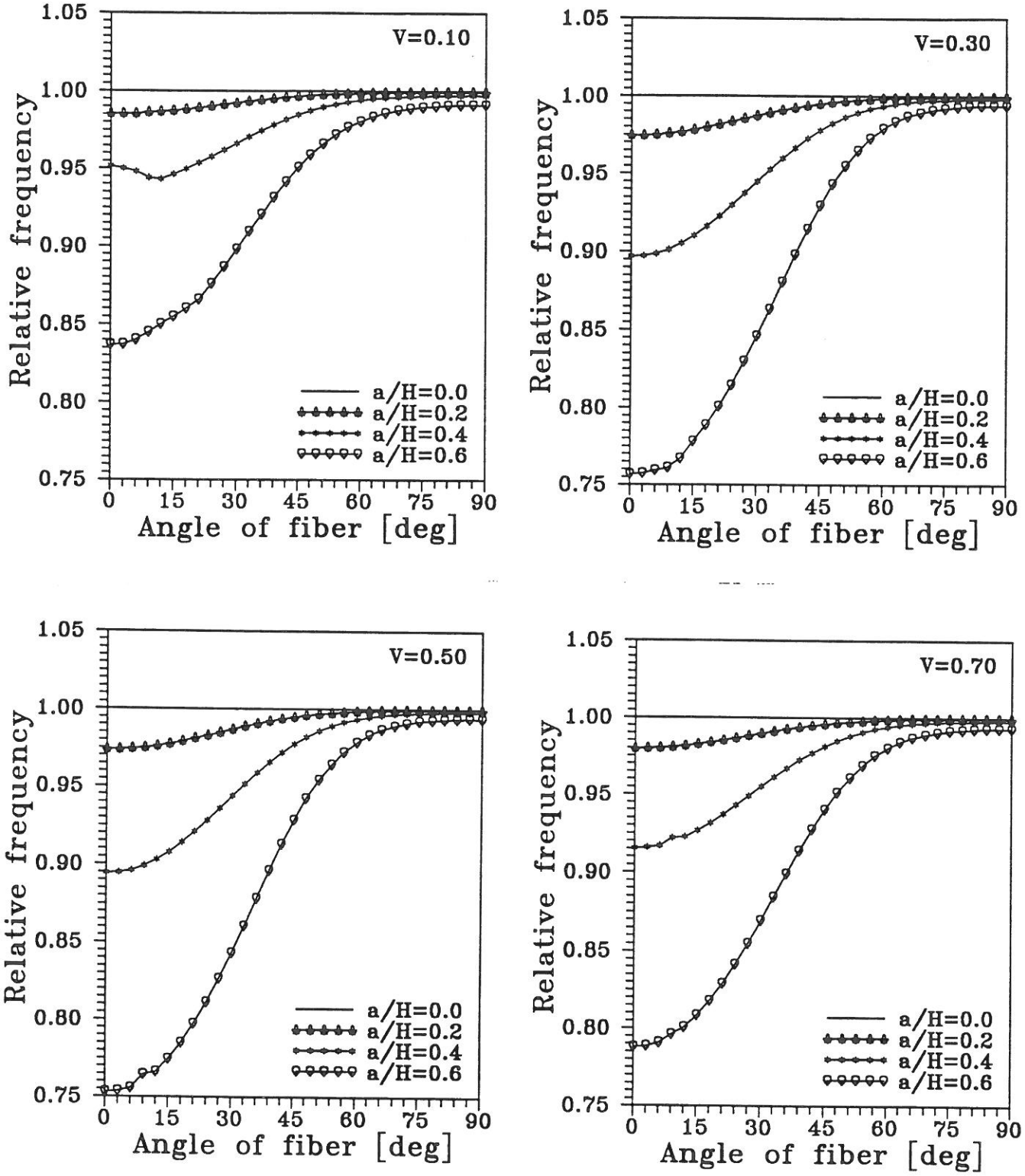

Fig.11

The relative changes of the first bending natural frequency of the beam as a function of the relative depth of crack and the angle of fiber, for several values of the volume fraction of fiber, are shown in Fig.11. The changes are normalized according with the following relation

$$\omega_r = \frac{\omega_c(\alpha)}{\omega_{nc}(\alpha)} , \tag{31}$$

where $\omega_c(\alpha)$ denotes the first bending natural frequency of the cracked beam as a function of the angle of fiber, $\omega_{nc}(\alpha)$ denotes the first bending natural frequency of the noncracked beam as a function of the angle of fiber.

The decrease of the fundamental bending natural frequency is strongest for the crack perpendiculars to the fiber direction. When, the angle of fiber increases this effect decreases and for the angle greater than 45 deg., the first bending natural frequency of the cracked beam has the same value like in the case of the noncracked beam (even for relatively depth crack - a/H=0.4).

Fig.12 shows the influence of the volume fraction of fiber on relative changes of the first bending frequency of the analyzed beam. In this case the relative changes of the natural frequency are calculating as

$$\omega_r = \frac{\omega_c(V)}{\omega_{nc}(V)} , \tag{32}$$

where $\omega_c(V)$ denotes the first bending natural frequency of the cracked beam as a function of the volume fraction of fiber, $\omega_{nc}(\alpha)$ denotes the first bending natural frequency of the noncracked beam as a function of the volume fraction of fiber.

The decrease of the first bending natural frequency is a function of the volume fraction of fiber. The maximum value is achieved at relatively higher fiber fractions (around 40%).

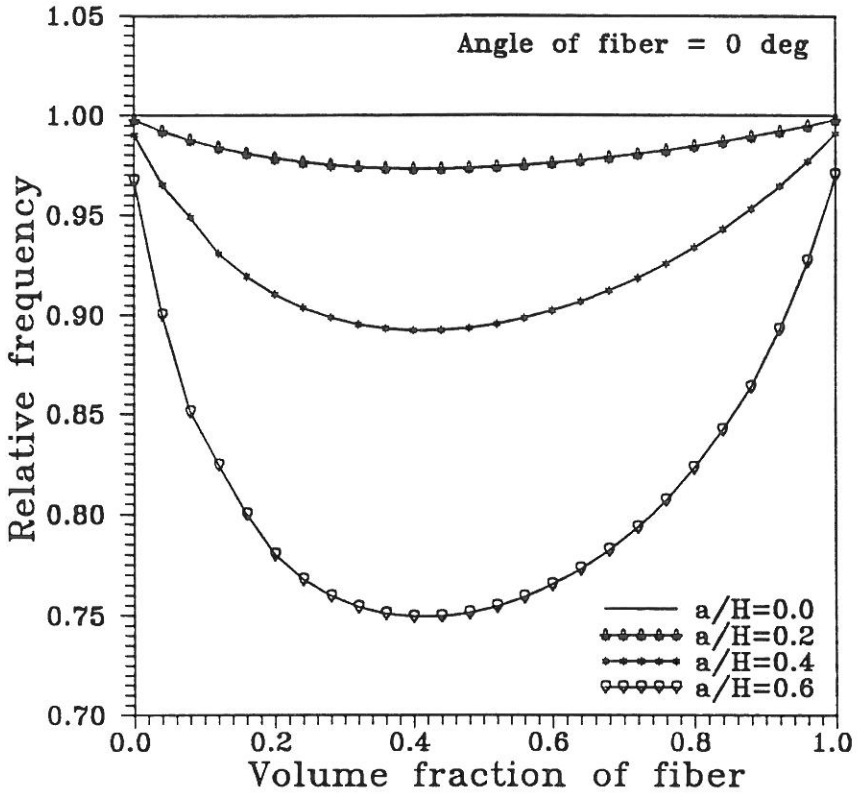

Fig.12

9. CONCLUSIONS

The paper presents a new beam finite element with the transverse nonpropagating one-edge open crack situated in the middle of its length. The element is versatile and can be used for static and dynamic analysis of composite or isotropic beam-like structures. In all cases, the results obtained with use of the element are satisfactory. The compatibility of the element with most plate and shell elements as a stiffener is apparent due its simple nodal variables of C^0-type. The method of creating the element, makes it possible to construct beam finite elements with various type of cracks (double-edge, internal etc.) if the stress intensity factors for a given type of crack are known.

The crack in the cantilever composite beam causes, as it was easily be expected, a increase of the static deflection and a reduce of the first bending natural frequency of its. These changes are a function not only the depth of the crack (like in the case of isotropic materials), but also the volume fraction of fiber and the angle of fiber. The

intensity of changes increases in accord with the increase of the depth of the crack. The changes of the static deflection and the fundamental natural frequency are largest when the volume fraction of fiber is equal to 40% and the crack is perpendicular to the fibers of the composite. For the angle of fiber greater than 45 deg. the static deflection and the first bending natural frequency have the similar value like in the case of the noncracked beam, (for all values of the volume fraction of fiber).

10. ACKNOWLEDGEMENTS

A partial support of the Danish Ministry of Education is gratefully acknowledged. The author greatly appreciate a possibility of using the computer hardware of Department of Building Technology and Structural Engineering the University of Aalborg.

REFERENCES

1. J.R. Vinson and T.W. Chou, *Composite Materials and Their Use in Structures*. Halsted Press Book, John Wiley and Sons, London (1975)
2. G.R. Irwin, Analysis of stresses and strains near the end of a crack transversing a plate. *Journal of Applied Mechanics* **24**, 361-364 (1956)
3. J. Wauer, Dynamics of cracked rotors: a literature survey. *Journal Applied Mechanics Review* **17**, 1-7 (1991)
4. R.D. Adams, P. Cawley, C.J. Pye and J. Stone, A vibration testing for non-destructively assessing the integrity of the structures. *Journal of Mechanical Engineering Sciences* **20**, 93-100 (1978)
5. P. Cawley and R.D. Adams, A vibration technique for non-destructive testing of fiber composite structures. *Journal of Composite Materials* **13**, 161-175 (1979)
6. K. Nikpour and A.D. Dimarogonas, Local compliance of composite cracked bodies. *Journal of Composite Science and Technology* **32**, 209-223 (1988)
7. K. Nikpour, Buckling of cracked composite columns. *Journal Solids Structures* **26**, 1371-1386 (1990)
8. S. Manivasagam and K. Chandrasekaran, Characterization of damage progression in layered composites. *Journal of Sound and Vibration* **152**, 177-179 (1992)
9. S. Oral, A shear flexible finite element for nonuniform, laminated composite beams. *Computers and Structures* **38**, 353-360 (1991)
10. A. Tessler and S.B. Dong, On a hierarchy of conforming Timoshenko beam elements. *Computers and Structures* **14**, 335-344 (1981)

11.O.C. Zienkiewicz, *The Finite Element Method,* McGraw-Hill, London (1991)

12.J.S. Przemieniecki, *Theory of Matrix Structural Analysis,* McGraw-Hill, London (1967)

13.M. Krawczuk and W.M. Ostachowicz, Hexahedral finite element with an open crack, to appear in *Finite Element Analysis and Design* (1993)

14.M. Krawczuk, Rectangular plate finite element with an open crack, to appear in *Computers and Structures* (1993)

15.H. Tada, P.C. Paris and G.R. Irwin, *The Stress Analysis of Cracks Handbook.* Del Research, St. Louis (1985)

16.G. Bao, S. Ho, Z. Suo and B. Fan, The role of material orthotropy in fracture specimens for composites. *Journal Solids Structures* **29**, 1105-1116 (1992)

17.S.G. Lekhnitskii, *Theory of Elasticity of an Anisotropic Body.* Mir Publishers, Moscow (1989)

18.J.R. Vinson and R.L. Sierakowski, *Behaviour of Structures Composed of Composite Materials.* Martinus Nijhoff Publishers, Dordrecht (1991)

19.G.C. Sih and E.P. Chen, Cracks in composite materials, in *Mechanics of Fracture.* Martinus Nijhoff Publishers, London (1981)

APPENDIX A

The properties of the graphite-fiber reinforced polyimide composite analyzed in the paper are assumed as follows [18]

Modulus of Elasticity: E_m = 2.756 GPa, E_f = 275.6 GPa,

Poisson Ratio: ν_m = 0.33, ν_f = 0.2,

Modulus of Rigidity: G_m = 1.036 GPa, G_f = 114.8 GPa,

Mass Density: ρ_m = 1600 kg/m^3, ρ_f = 1900 kg/m^3,

where m denotes the matrix whereas f denotes the fiber.

The material is assumed orthotropic with respect to its axes of symmetry which lie along and perpendicular to the direction of fibers. The gross mechanical properties of the composite are calculated using the following formulas [18]

$$\rho = \rho_f v + \rho_m(1-v) ,$$

$$E_{11} = E_f v + E_m(1-v) \ ,$$

$$E_{22} = E_m \left[\frac{E_f + E_m + (E_f - E_m)v}{E_f + E_m - (E_f - E_m)v}\right] \ ,$$

$$\nu_{12} = \nu_f v + \nu_m(1-v) \ ,$$

$$\nu_{23} = \nu_f v + \nu_m(1-v)\left[\frac{1 + \nu_m - \nu_{12}E_m/E_{11}}{1 - \nu_m^2 + \nu_m\nu_{12}E_m/E_{11}}\right] \ ,$$

$$G_{12} = G_m \left[\frac{G_f + G_m + (G_f - G_m)v}{G_f + G_m - (G_f - G_m)v}\right] \ ,$$

$$G_{23} = \frac{E_{22}}{2(1 + \nu_{23})} \ ,$$

where v denotes the volume fraction of fiber.

The principal axes 1 and 2 are in the plane of the composite specimen aligned along and perpendicular to the fibers directions.

APPENDIX B

The complex constants s_1 and s_2 in relations (20.a-c) are roots of the following characteristic equation [19]

$$\bar{b}_{11}s^4 - 2\bar{b}_{16}s^3 + (2\bar{b}_{12} + \bar{b}_{66})s^2 - 2\bar{b}_{26}s + \bar{b}_{22} = 0 \ .$$

The constant $\bar{b}_{ij}$ are calculated from the following relations [19]

$$\bar{b}_{11} = b_{11}m^4 + (2b_{12} + b_{66})m^2n^2 + b_{22}n^4 \ ,$$

$$\bar{b}_{22} = b_{11}n^4 + (2b_{12} + b_{66})m^2n^2 + b_{22}m^4 \ ,$$

$$\bar{b}_{12} = (b_{11} + b_{22} - b_{66})m^2n^2 + b_{12}(m^4 + n^4) ,$$

$$\bar{b}_{16} = (-2b_{11} + 2b_{12} + b_{66})m^3n + (2b_{22} - 2b_{12} - b_{66})mn^3 ,$$

$$\bar{b}_{26} = (-2b_{11} + 2b_{12} + b_{66})n^3m + (2b_{22} - 2b_{12} - b_{66})nm^3 ,$$

$$\bar{b}_{66} = 2(2b_{11} - 4b_{12} + 2b_{22} - b_{66})m^2n^2 + b_{66}(m^4 + n^4) ,$$

where $m = \cos\alpha$, $n = \sin\alpha$ (α denotes the angle between geometric axes of the beam and the material principal axes) - see Fig.1.

The terms b_{ij} corresponds with the situation when geometric axes of the beam coincide with material principal axes. These are related to the mechanical constants of the material by [19]

$$b_{11} = \frac{1}{E_{11}}\left(1 - \nu_{12}^2 \frac{E_{22}}{E_{11}}\right) ,$$

$$b_{22} = \frac{1}{E_{22}}\left(1 - \nu_{23}^2\right) ,$$

$$b_{12} = \frac{-\nu_{12}}{E_{11}}\left(1 + \nu_{23}\right) ,$$

$$b_{66} = \frac{1}{G_{12}} .$$

The roots of the characteristic equation are either complex or pure imaginary and cannot be real. Thus, the four roots separate into two sets of distinct complex conjugates. The parameters s_1 and s_2 correspond to those with positive imaginary parts. The roots of characteristic equation were computed with an accuracy of 10^{-10} using Newton-Raphson method for polynomial equations with complex roots.

APPENDIX C

In the case of the analyzed element, the stress-strain relation matrix posses the form [18]

$$\mathbb{D} = \left[\begin{array}{c|c} \bar{S}_{11} & \bar{S}_{16} \\ \hline \bar{S}_{16} & \bar{S}_{66} \end{array}\right]$$

where [18]

$$\bar{S}_{11} = S_{11}m^4 + 2(S_{12} + 2S_{66})m^2n^2 + S_{22}n^4 ,$$

$$\bar{S}_{16} = (S_{11} - S_{12} - 2S_{66})m^3n + (S_{12} - S_{22} + 2S_{66})mn^3 ,$$

$$\bar{S}_{66} = (S_{11} - 2S_{12} + S_{22} - 2S_{66})m^2n^2 + S_{66}(m^4 + n^4) .$$

The terms S_{ij} corresponding with the material principal axes are determined from the following relations [18]

$$S_{11} = \frac{E_{11}}{1 - \nu_{12}^2 \frac{E_{22}}{E_{11}}} ,$$

$$S_{22} = S_{11} \frac{E_{22}}{E_{11}} ,$$

$$S_{12} = \nu_{12} S_{22} ,$$

$$S_{66} = G_{12} .$$

LIST OF FIGURES

FRACTURE AND DYNAMICS PAPERS

PAPER NO. 13: Lise Gansted: *Fatigue of Steel: Deterministic Loading on CT-Specimens.*

PAPER NO. 14: Jakob Laigaard Jensen, Rune Brincker & Anders Rytter: *Identification of Light Damping in Structures.* ISSN 0902-7513 R8928.

PAPER NO. 15: Anders Rytter, Jakob Laigaard Jensen & Lars Pilegaard Hansen: *System Identification from Output Measurements.* ISSN 0902-7513 R8929.

PAPER NO. 16: Jens Peder Ulfkjær: *Brud i beton - State-of-the-Art. 1. del, brudforløb og brudmodeller.* ISSN 0902-7513 R9001.

PAPER NO. 17: Jakob Laigaard Jensen: *Full-Scale Measurements of Offshore Platforms.* ISSN 0902-7513 R9002.

PAPER NO. 18: Jakob Laigaard Jensen, Rune Brincker & Anders Rytter: *Uncertainty of Modal Parameters Estimated by ARMA Models.* ISSN 0902-7513 R9006.

PAPER NO. 19: Rune Brincker: *Crack Tip Parameters for Growing Cracks in Linear Viscoelastic Materials.* ISSN 0902-7513 R9007.

PAPER NO. 20: Rune Brincker, Jakob L. Jensen & Steen Krenk: *Spectral Estimation by the Random Dec Technique.* ISSN 0902-7513 R9008.

PAPER NO. 21: P. H. Kirkegaard, J. D. Sørensen & Rune Brincker: *Optimization of Measurements on Dynamically Sensitive Structures Using a Reliability Approach.* ISSN 0902-7513 R9009.

PAPER NO. 22: Jakob Laigaard Jensen: *System Identification of Offshore Platforms.* ISSN 0902-7513 R9011.

PAPER NO. 23: Janus Lyngbye & Rune Brincker: *Crack Length Detection by Digital Image Processing.* ISSN 0902-7513 R9018.

PAPER NO 24: Jens Peder Ulfkjær, Rune Brinker & Steen Krenk: *Analytical Model for Complete Moment-Rotation Curves of Concrete Beams in bending.* ISSN 0902-7513 R9021.

PAPER NO 25: Leo Thesbjerg: *Active Vibration Control of Civil Engineering Structures under Earthquake Excitation.* ISSN 0902-7513 R9027.

PAPER NO. 26: Rune Brincker, Steen Krenk & Jakob Laigaard Jensen: *Estimation of correlation Functions by the Random Dec Technique.* ISSN 0902-7513 R9028.

PAPER NO. 27: Jakob Laigaard Jensen, Poul Henning Kirkegaard & Rune Brincker: *Model and Wave Load Identification by ARMA Calibration.* ISSN 0902-7513 R9035.

PAPER NO. 28: Rune Brincker, Steen Krenk & Jakob Laigaard Jensen: *Estimation of Correlation Functions by the Random Decrement Technique.* ISSN 0902-7513 R9041.

FRACTURE AND DYNAMICS PAPERS

PAPER NO. 29: Poul Henning Kirkegaard, John D. Sørensen & Rune Brincker: *Optimal Design of Measurement Programs for the Parameter Identification of Dynamic Systems.* ISSN 0902-7513 R9103.

PAPER NO. 30: L. Gansted & N. B. Sørensen: *Introduction to Fatigue and Fracture Mechanics.* ISSN 0902-7513 R9104.

PAPER NO. 31: R. Brincker, A. Rytter & S. Krenk: *Non-Parametric Estimation of Correlation Functions.* ISSN 0902-7513 R9120.

PAPER NO. 32: R. Brincker, P. H. Kirkegaard & A. Rytter: *Identification of System Parameters by the Random Decrement Technique.* ISSN 0902-7513 R9121.

PAPER NO. 33: A. Rytter, R. Brincker & L. Pilegaard Hansen: *Detection of Fatigue Damage in a Steel Member.* ISSN 0902-7513 R9138.

PAPER NO. 34: J. P. Ulfkjær, S. Krenk & R. Brincker: *Analytical Model for Fictitious Crack Propagation in Concrete Beams.* ISSN 0902-7513 R9206.

PAPER NO. 35: J. Lyngbye: *Applications of Digital Image Analysis in Experimental Mechanics.* Ph.D.-Thesis. ISSN 0902-7513 R9227.

PAPER NO. 36: J. P. Ulfkjær & R. Brincker: *Indirect Determination of the $\sigma - w$ Relation of HSC Through Three-Point Bending.* ISSN 0902-7513 R9229.

PAPER NO. 37: A. Rytter, R. Brincker & P. H. Kirkegaard: *An Experimental Study of the Modal Parameters of a Damaged Cantilever.* ISSN 0902-7513 R9230.

PAPER NO. 38: P. H. Kirkegaard: *Cost Optimal System Identification Experiment Design.* ISSN 0902-7513 R9237.

PAPER NO. 39: P. H. Kirkegaard: *Optimal Selection of the Sampling Interval for Estimation of Modal Parameters by an ARMA-Model.* ISSN 0902-7513 R9238.

PAPER NO. 40: P. H. Kirkegaard & R. Brincker: *On the Optimal Location of Sensors for Parametric Identification of Linear Structural Systems.* ISSN 0902-7513 R9239.

PAPER NO. 41: P. H. Kirkegaard & A. Rytter: *Use of a Neural Network for Damage Detection and Location in a Steel Member.* ISSN 0902-7513 R9245

PAPER NO. 42: L. Gansted: *Analysis and Description of High-Cycle Stochastic Fatigue in Steel.* ISSN 0902-7513 R9135.

PAPER NO. 43: M. Krawczuk: *A New Finite Element for Static and Dynamic Analysis of Cracked Composite Beams.* ISSN 0902-7513 R9305.

Department of Building Technology and Structural Engineering
The University of Aalborg, Sohngaardsholmsvej 57, DK 9000 Aalborg
Telephone: 45 98 15 85 22 Telefax: 45 98 14 82 43